A single-photon avalanche camera for fluorescence lifetime imaging microscopy and correlation spectroscopy

Marco Vitali, Danilo Bronzi, Aleksandar J. Krmpot, Stanko Nikolić, Franz-Josef Schmitt, Cornelia Junghans, Simone Tisa, Thomas Friedrich, Vladana Vukojević, Lars Terenius, Franco Zappa, *Senior Fellow, IEEE* and Rudolf Rigler

***Abstract*—Confocal Laser Scanning Microscopy (CLSM) is commonly used to observe molecules of biological relevance in their native environment, the live cell, and study their spatial distribution and interactions. CLSM can be easily extended to measure the lifetime of the excited state of fluorescent molecules and their diffusion properties, with Fluorescence Lifetime Imaging Microscopy (FLIM) and Fluorescence Correlation Spectroscopy (FCS), in order to provide additional information about the cell biochemistry. However, these physical parameters cannot be measured simultaneously using conventional CLSM at very high scanning speeds due to photodamage and saturation of the fluorescence signal of the excited molecules or induced phototoxicity to the observed biosystems. To overcome these limitations, we developed a new camera that consists of 1024 Single-Photon Avalanche Diodes (SPADs) which is optimized for multifocal microscopy, FLIM and FCS. We show proof-of-principle measurements of fluorescence intensity distribution and lifetime of the enhanced Green Fluorescent Protein (eGFP) expressed in live cells and measurement of Quantum Dots (QD) diffusion in solution by FCS using the same detector.**

***Index Terms*—Single Photon Avalanche Diode array, Multifocal microscopy, Fluorescence Lifetime Imaging Microscopy, Fluorescence Correlation Spectroscopy.**

I. Introduction

CONFOCAL Laser Scanning Microscopy (CLSM) is universally used in biomedical research to investigate molecular mechanisms underlying vital biological functions. CLSM primarily owes its widespread use to its capacity to produce sharp images of structures in vivo. This is achieved through a special arrangement of optical elements, which focus the laser beam in a diffraction-limited volume of about 1 fL, depending on the excitation wavelength, and detect fluorescence from an even smaller volume by filtering the emitted light through a pinhole, a circular aperture of few tens of micrometers in diameter that is placed in front of the detector. Through this special optical arrangement, a fluorescence signal is detected only from molecules that are confined in this small, so-called confocal volume. The fluorescence emission from outer molecules is strongly attenuated by the pinhole, thus enabling the selective observation of a subset of fluorophores at a high signal-to-noise ratio [1].

An important feature of confocal microscopy is the possibility to visualize the three-dimensional spatial distribution of molecules of interest within the investigated specimen. This is achieved by raster-scanning the confocal volume either by steering the laser beam using fast galvanometric scanners and acousto-optic deflectors, or by moving the sample using nanopositioning piezoelectric microscope stages.

Confocal laser scanning microscopes achieve image acquisitions at rates of about 30 frames per second (fps) or more in fast scanning modes [2]. Under these operating conditions, a relatively high illumination intensity is needed since the dwell time per pixel is 10^4 to 10^6 times shorter than the acquisition time required for a single frame. Acquisitions at higher frame-rates are possible with the currently available instrumentation but the intensity of the excitation beam has to be strongly increased to facilitate signal acquisition at very short times. For this reason, photodamage of the observed fluorophore and photoxicity of the investigated biosystems might be fostered by nonlinear processes [3]. Additionally, the absorption of the fluorophores might even reach saturation levels, and further increase in the illumination intensity does not improve significantly the signal but rather increases the optical background noise.

These limitations were solved by constructing multifocal microscopes, where multiple confocal volumes are simultaneously scanned over the sample. Indeed, the use of the massively parallel confocal arrangements permits to acquire a full frame at the acquisition time of a single pixel in classical CLSM. Hence, fast acquisition rates are achieved without increasing the illumination power as a result of the longer dwell times per pixel. Line-scanning and spinning disk

M. Vitali was with the Department of Chemistry, Berlin Institute of Technology, Berlin 10623, Germany. He is now with the company Omicron Energy Solutions GmbH, Berlin, Germany (Email: marco.vitali@omicron.at).

F.-J. Schmitt, C. Junghans and T. Friedrich are with the Department of Chemistry, Berlin Institute of Technology, Berlin 10623, Germany. (Email: schmitt@physik.tu-berlin.de; cornelia.junghans@tu-berlin.de, friedrich@chem.tu-berlin.de)

D. Bronzi and F. Zappa are with the Dipartimento di Elettronica e Informazione, Politecnico di Milano, Milano 20133, Italy (Email: danilo.bronzi@elet.polimi.it; franco.zappa@polimi.it).

S. Tisa is with Micro Photon Device srl, Bolzano 39100, Italy (Email: stisa@micro-photon-devices.com).

A. Krmpot and S. Nikolic are with Institute of Physics, University of Belgrade, Pregrevica, Belgrade 11080, Serbia (Email: krmpot@ipb.ac.rs; stankon@ipb.ac.rs).

V. Vukojevic and L. Terenius are with Department of Clinical Neuroscience, Karolinska Institutet, Stockholm 17176, Sweden (Email: Vladana.Vukojevic@ki.se; Lars.Terenius@ki.se).

R. Rigler is with Department of Medical Biochemistry and Biophysics, Karolinska Institutet, Stockholm 17176, Sweden (Corresponding author; phone: +46-708458694; Email: Rudolf.Rigler@ki.se).

confocal systems achieves up to 1000 fps [1], [4] and two-dimensional detector arrays such as Electron-Multiplying CCD cameras or CMOS sensors are commonly used to measure the fluorescence signal. Fast frame-rate microscopy techniques have a huge potential for biological investigations. An improvement of the frame acquisition speed up to 10-100 kfps would allow the characterization of protein diffusion processes in live cells.

A standard tool to investigate the mobility of molecules and proteins in living organisms is Fluorescence Correlation Spectroscopy (FCS). In FCS, temporal autocorrelation analysis is applied to detect nonrandomness in the fluctuations of the fluorescence signal. This technique is therefore able to monitor all processes that lead to fluorescence intensity fluctuations at the temporal scale between few tens of nanoseconds up to seconds or longer e.g. formation of triplet and dark states, Brownian motion, protein-protein interactions and liquid flow [5]. On the other hand, classical FCS experimental setups are mostly limited to the observation of a single confocal volume and they cannot investigate simultaneously multiple regions in the sample. The construction of a multifocal microscopy setup which is capable of fast frame-rates above 10 kfps is, therefore, of major scientific interest. Not only the intensity of the fluorescence emission signal would be observed, but also its fast fluctuations as a function of the position within the sample, enabling parallel FCS studies across a cell.

The design of suitable bidimensional photodetectors plays a key role for the implementation of the described multifocal system. The acquisition speed is not the only important parameter, but also the Photon Detection Efficiency (PDE), dark signal and saturation levels are limiting factors. High-gain solid-state detectors as the Single Photon Avalanche Photodiode (SPAD) have all these properties. A fair PDE above 40% and few thousands dark counts per second (cps) are commonly specified [6]–[8]. Saturation rates in the order of many millions of photons per second are possible [7]. Additionally, SPADs are not affected by any read-out noise, in contrast to CCD or CMOS sensors, which is a major advantage to combine high frame-rate imaging and FCS. In fact, the frames acquired at 10 to 100 kfps, which are required for FCS, are consecutively binned over time, e.g. few milliseconds, to visualize the spatial distribution of the measured fluorophores. This binning operation is performed during post-processing of the data and it does not degrade the signal-to-noise ratio due to the absence of read-out noise.

Several pioneering works investigated the use of multifocal FCS experimental setups more than 10 years ago [9]–[11]. The number of SPADs and confocal volumes was not sufficiently large to allow for the reconstruction of images, although the main experimental concepts were already developed. More recent works used the next generation SPAD imagers featuring 1024 photodetectors on the same silicon chip [12]–[15].

We present a new 32×32 SPAD camera which fulfills all the requirements indicated above, which make it suitable for a multifocal FCS experimental setup. This device implements additionally a fast time-gating control, which enables the pixel electronics for short time periods down to 1.5 ns at delay steps below 100 ps. This camera is therefore capable of measuring not only the fluctuations of the fluorescence intensity at very high frame-rates (50 kHz to 100 kHz) but also the decay kinetics of fluorophores after illumination by a pulsed laser. Combined with a multifocal optical setup, this system is readily extended into a time-gated Fluorescence Lifetime Imaging Microscopy (FLIM) [16]–[18] experimental setup. The measurement of fluorescence decay kinetics by each SPAD allows the monitoring of ultra-fast photophysical processes as the Förster Resonance Energy Transfer (FRET) and to identify multiple fluorescence sources. In summary, the multifocal FLIM/FCS setup combines three of the most important microscopy techniques in a single system. We validated the proposed camera using several model experiments such as the measurement of the diffusion time of single Quantum Dots (QD) in solution and the fluorescence decay kinetics of genetically encoded enhanced Green Fluorescent Protein (eGFP) expressed in live cells.

II. Camera design

The camera design optimized for multifocal microscopy was based on an array of 1024 independent SPADs produced in standard CMOS technology [7], [19], [20]. The detectors were organized in a 32×32 array of smart pixels, featuring both photodetection circuitry and pre-processing electronics (Fig. 1-a). The physical dimension of the pixel was 100 μm $\times$ 100 μm, while the circular active area had a diameter of 20 μm.

The SPAD [21] is a reverse-biased pn junction, which is operated well above its breakdown voltage. Under this biasing condition the absorption of a single photon, causes the generation of an electron-hole pair, which is accelerated by the electric field across the junction. The energy of the charge carriers is eventually sufficient to trigger a self-sustained macroscopic avalanche current of few milliamperes through the device.

A quenching circuit based on a time-varying active load (Variable-Load Quenching Circuit, VLQC) [22] has been integrated for sensing the SPAD ignition, quenching the avalanche and resetting the detector to its initial condition. Compared to quenching circuits based on passive loads, the VLQC has the major advantage of speeding up the quenching action, thus minimizing the charge amount which flows through the SPAD after ignition. Moreover, a fixed dead-time, i.e. the minimum time interval between two detection events, of several tens of nanoseconds is externally set.

The use of SPADs as photodetectors has major advantages for imaging applications concerning the signal-to-noise ratio. No analog measurement of voltage or current is needed, since the detector acts as a digital Geiger-like counter. Hence, no read-out noise is added to the measurement process. This is a very important advantage for high-frame rate microscopy imaging, since the probability of detecting a single photon per frame and per pixel is usually low ($\ll$1). A second major advantage of the presented pixel structure concerns the short dead-time, which has a lower limit of about 50 ns. This rises the maximum number of photons which are processed per second.

The dominant noise processes for the described pixels were dark counts generation and afterpulsing [19]. The former was

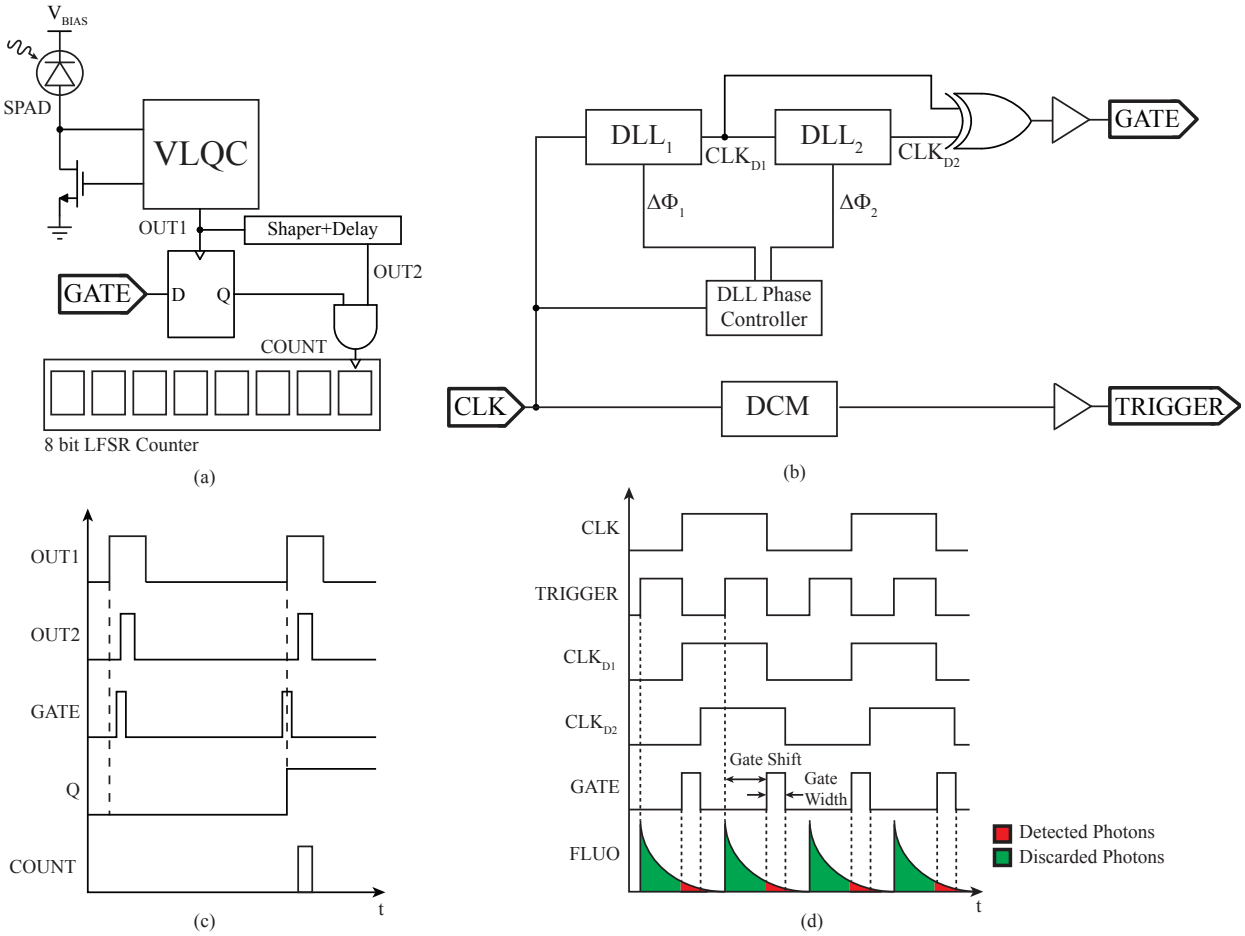

Figure 1. (a) Scheme of the smart pixel architecture. (b) Timing signals within the pixel architecture. (c) Architecture for the generation of the fast gate signal by a Spartan 6 FPGA devices. (d) Scheme of the Time-Gated FLIM experiment.

below 4.000 cps for more than 75% of the total number of pixels at room temperature and at +5 V excess bias. The remaining ones showed values between tens to several hundredths thousands counts per seconds.

Afterpulsing depends strongly on the overvoltage and dead-time values. In this study, the dead time was set to 200 ns, and the afterpulsing probability achieved a maximum of 5% over the whole array. It increased above 20% if the dead-time was set to 50 ns, which is the lower limit for the current hardware design. On the other hand, the PDE at the defined overvoltage was above 40% at 450 nm, and it decreased to about 27% at 550 nm.

Fig. 1-a provides a schematic view of the pixel architecture. The VLQC output, which is synchronous with the avalanche sensing, triggers the processing electronics and an 8-bit Linear-Feedback Shift-Register (LFSR) counts the detection events. Routing electronics is then implemented on the same chip to read-out the counter values and to transfer them to the off-chip electronics. This design allows the measurements of 50.000 to 100.000 frames per second. The presented architecture additionally allows gating of the LFSR counters for a very short time between 1.5 ns and 20 ns. In this way, the trigger signal by the VLQC circuit increments the LFSR counter only when the signal GATE is asserted (logic level '1'). Otherwise, the detected photons are not counted (logic level '0'). To reach gated photon counting within each pixel, the output pulse from the quenching circuit (OUT1) is used to clock a D-Flip-Flop (D-FF), which samples the signal GATE generated by the camera electronics. OUT1 is additionally delayed, reshaped and sent to an AND gate to properly drive the counter. Fig. 1-c shows the timing diagram of the counting circuitry when the fast gate signal is applied.

In order to keep the architecture as flexible as possible, the generation of the GATE signal was performed by an external Field Programmable Gate Array (FPGA) (Spartan 6, XC6SLX45-2FGG484 Xilinx, San Jose, CA, USA). A Xem6010 (Opal Kelly, Portland, OR, USA) development board, which incorporates both the Spartan 6 FPGA and a high speed USB 2.0 interface, was used to control the read-out of the chip and to transfer the measured images to the host computer.

Fig. 1-b shows the architecture based on the internal Delay Locked Loops (DLLs) of the FPGA device, which were used to generate fast gate signals. FPGA devices require DLLs to de-skew the internal digital paths and to fine-tune the sampling time of fast serial communication lines. They are designed to produce a precise phase shift between 10 and 40 ps, which can be dynamically controlled during operation. The update of the

DLL shift requires few tens of clock cycles in the worst case, i.e. few microseconds depending on the used FPGA family. This dynamic phase shift is, therefore, well suited to generate periodic sequences of pulses. Fig. 1-d shows how de-phased clock signals are combined to generate pulses of variable width. The 50 MHz to 100 MHz board clock (CLK), which is used to synchronize and control the camera operations, is sent to DLL_1 and shifted of a fixed delay $\Delta\Phi_1$. This clock signal, $\mathrm{CLK}_{\mathrm{D1}}$, is sent to a second DLL (DLL_2) which creates an additional phase shifted clock ($\Delta\Phi_2$, $\mathrm{CLK}_{\mathrm{D2}}$). The XOR between $\mathrm{CLK}_{\mathrm{D1}}$ and $\mathrm{CLK}_{\mathrm{D2}}$ creates short pulses of variable width and at a repetition rate which is twice the clock frequency (GATE). The phase difference between CLK and $\mathrm{CLK}_{\mathrm{D1}}$ will be referred to in the text as *gate shift* while the phase between $\mathrm{CLK}_{\mathrm{D1}}$ and $\mathrm{CLK}_{\mathrm{D2}}$ will be denoted *gate width*. Both *gate shift* and *gate width* are dynamically adjusted during data acquisition.

This logic design was implemented to set up a time-gated FLIM detection system [18]. The board clock is frequency doubled by a Digital Clock Manager (DCM) and used as a trigger signal for a pulsed laser diode (TRIGGER) (Fig. 1-b,d). The generated laser pulses are coupled to a wide-field fluorescence microscope, as described in section V-A, and used to illuminate the sample. The laser radiation is absorbed by fluorescent molecules which are electronically excited. During relaxation into the ground state, the molecules emit fluorescence photons with a certain probability, which are then measured by the camera. The GATE signal activates the LFSR counters after the generation of the laser pulse for the time defined by *gate width* (Fig. 1-c, red color). Accordingly, the fluorescence decay kinetics is measured by changing *gate shift* over time. Both *gate shift* and *gate width* have optimal values depending on the lifetime of the excited state of the fluorescent molecules and on the imaging frame-rate [23], [24]. For simplicity, we used a constant *gate width* and incremented *gate shift* by fixed steps between 100 ps and 500 ps.

In summary, the presented camera architecture is a trade-off between accurate time measurements on the timescale of few nanoseconds and fast processing of the measured signals up to the limit of millions of photons per second and pixel. Any detector that is suitable for both FLIM and FCS experiments must fulfill these requirements.

III. Multifocal Microscopy Setup

The multifocal FLIM/FCS setup was built on a standard Axio Observer D1 inverted microscope (Zeiss, Jena, Germany) equipped with a C-Apochromat 63×/1.2 W. Corr. objective (Zeiss, Jena, Germany). The filter setting for eGFP (Ex. band-pass 470/40, beam splitter FT 495, Em. band-pass 525/50) was used. The optical pathway scheme is shown in Fig. 2. Two laser sources were used for the experiments. For FCS measurement, a CW diode laser (Excelsior 488, Newport-Spectra Physics, Darmstadt, Germany) was used. Its fundamental emission wavelength at 976 nm was frequency doubled at 488 nm and a beam quality factor smaller than 1.1 at a power of 80 mW was obtained. For lifetime imaging microscopy, a

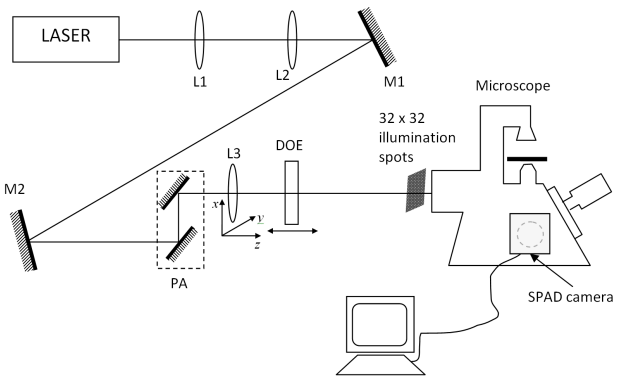

Figure 2. Scheme of the optical setup used for the creation of the 32×32 confocal volumes. Lenses L1, L2, and L3, mirrors M1 and M2 and Periscope Assembly (PA). The Diffractive Optical Element (DOE) and lens L3 were used to project an illumination array at the image plane of the microscope.

pulsed laser diode (LDH-475, Picoquant, Berlin, Germany) with pulses shorter than 100 ps FWHM, a repetition rate of 50 MHz and total average power of about 1 mW was used. The laser beam was firstly attenuated by neutral density filters and then expanded by a factor of 10 using a telescope (L1 and L2). The beam height from the optical table was adjusted by a periscope assembly (PA) to enter the back illumination port of the microscope. The expanded beam was then re-focused by lens L3 (focal length 150 mm). Immediately after, the beam passed through a Diffractive Optical Element (DOE) (Holoeye, Berlin, Germany) in order to create a array of 32×32 spots with a pitch of 100 µm and a diameter of 12.5 µm at the image plane.

The DOE is a glass hologram designed to diffract a single laser beam into 1024 beams at different angles. The diffraction angles and the intensity of the zeroth order diffraction (transmitted beam) depends on the incident wavelength. The zero order beam, although not negligible, did not affect the performance of the system.

The sharpness of the spots projected on the image plane was adjusted by moving lens L3 along the optical axis. Other two micrometer stages were used to center the position of the array perpendicularly to the optical axis. The distance between the DOE position and the lens L3 was fine-tuned to match the pitch of the illumination spots and the active areas of the SPAD camera. The small diameter of the SPAD acts as a spatial filter and no additional pinholes are required in front of the detectors, in contrast with standard confocal microscopes. The previously described 32×32 SPAD camera (Micro-Photon-Devices, Bolzano, Italy) was connected to the side port of the microscope by a standard C-mount adapter. The acquired images were then transferred to the processing computer via a high-speed USB 2.0 interface. FCS imaging was performed using Visual SPC^2 acquisition software (Micro-Photon-Devices, Bolzano, Italy) and the frame-rate was set to values between 50 kHz to 100 kHz.

The acquisition of FLIM images required the optimization of the camera firmware to generate fast gate signals and the synchronization pulses to trigger the laser diode.

IV. Analysis of the data

The analysis of FLIM data acquired by time-gated techniques has been a subject of several works [25], [26] and more recently of a specialized review focusing on solid-state imaging sensors [24]. The data analysis method depends strongly on the gating scheme used, i.e. the selected values of *gate shift* and *gate width* as a function of the lifetime of the excited state of the observed fluorophores. The method described in [26] provides results close to the optimum for the gating scheme described in section II. Indeed, it is a Maximum Likelihood (ML) approach and it provides an unbiased estimation of the model parameter even for very low numbers of photons per pixel. Compared to other approaches like the least square technique, ML estimation is both more precise and accurate, as experimentally verified by Maus *et al.* [27]. This approach has only one drawback. It does not account for the uncorrelated noise present in the decay traces, e.g. due to room light or dark counts of the SPAD detectors. Therefore, background subtraction has to be applied before estimating the lifetimes.

The adopted method searches for the lifetime value τ which is the solution of the implicit equation

$$\frac{\sum_{i=1}^{k} i * x[i]}{\sum_{i=1}^{k} x[i]} = \frac{1}{exp(T/\tau) - 1} - \frac{k}{exp(k * T/\tau) - 1} + 1, \quad (1)$$

where x_i are the number of detected photons in the i$^{\text{th}}$ gate channel, T is the constant duration of the time channel, 0.18 ns for the described experiments, and m is the total number of channels. The estimated τ represents the average lifetime, when the observed fluorophores decay according to multi-exponential models ($m(t)$).

$$m(t) = \sum_{i=1}^{N_c} a_i exp\,(t/\tau_i) \quad (2)$$

$$< \tau >= \sum_{i=1}^{N_c} a_i \tau_i^2 \quad (3)$$

where a_i are the pre-exponential factors and τ_i the set of lifetimes.

While eq. 1 can be solved in less than 1 s for a whole FLIM image using Matlab (The MathWorks Inc., Natick, MA, USA), the FCS data analysis requires more optimized computational methods to be executed within few seconds. The standard algorithm to calculate the autocorrelation curves, which is usually known as Multi-τ algorithm or Schätzel method [28], [29], is computationally expensive. Indeed, millions of multiplications are needed to construct the Autocorrelation Curve (ACC) for each single pixel. The ACC, G(τ), is calculated from eq. 4

$$G(\tau) = \frac{< F(t)F(t+\tau) >}{< F(t) >^2} \quad (4)$$

where F(t) is the measured time-dependent fluorescence intensity, and <> denotes averaging over time [30].

Eq. 4 can be solved analytically for simple geometries and processes as the translational motion of freely diffusing fluorophores in solution [31]. The solution for this special case yields the Autocorrelation Function (ACF):

$$G(\tau) = G(0)\left(1 + \frac{\tau}{\tau_D}\right)^{-1}\left[1 + \left(\frac{s}{u}\right)^2 \frac{\tau}{\tau_D}\right]^{-1/2} \quad (5)$$
$$\tau_D = \frac{s^2}{4D}$$

where G(0) is the amplitude at $\tau = 0$, τ_D is the diffusion time, s and u are the radii of the confocal volume measured perpendicular to, and along the optical axis where the excitation intensity reaches e^{-2} of its value at the center of the confocal volume, and D is the diffusion constant of the investigated molecules in solution.

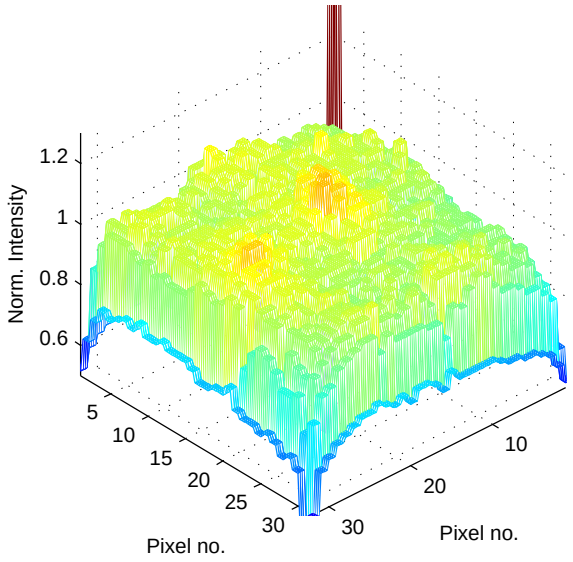

Figure 3. Illumination uniformity over the whole 32×32 SPAD array

We developed dedicated software both to communicate efficiently with the camera and to calculate the ACC for each pixel from sets of 130.000 images by massive parallelization of the calculation using a NVIDIA GeForce GTX 780 (NVIDIA corporation, Santa Clara, CA, USA) Graphical Processing Unit (GPU). This GPU board supports the CUDA parallel computing platform and it is capable of running tens of thousands of threads concurrently. Thereby, the computational time of the calculation of 1024 complete ACCs decreased to about 4 s, compared to the about 200 s execution time that was needed when using a single CPU. The parameters of the ACF (eq. 5) were calculated for each pixel. G_0 and τ_D were estimated by the value of the ACC at 41.4 µs and its full width at half maximum respectively.

It has been shown that both the estimation of lifetimes and the processing required for FCS data analysis can be embedded in the acquisition electronics [13], [32], [33]. These methods, thought excellent, are absolutely needed for real-time and high throughput applications, which are outside the scope of the current work. Future developments will focus on implementing similar algorithms for the described SPAD array architecture.

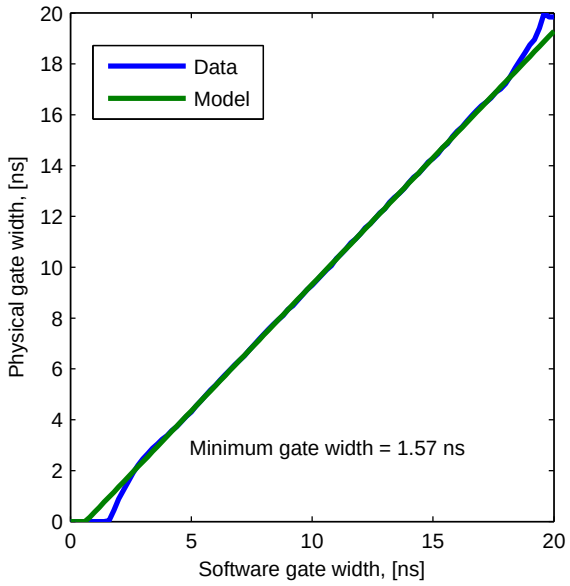

Figure 4. Linearity of the gate width as a function of the camera setting. Uncorrelated light from a stabilized LED was used to generate a constant light signal.

V. Experimental results

We applied the multifocal microscope in several model experiments to show the performance of the system. The results are divided in three sections concerning the microscopy setup, FLIM and FCS.

A. Microscopy setup

A first important test was to measure the uniformity of the system over the whole field of view after illumination by the DOE and detection using the SPAD camera. The uniformity of the experimental setup was measured by imaging an aqueous solution of Quantum Dots (QD, 525 ITK^{TM} Molecular Probes, Darmstadt Germany). The selected QDs emit around 525 nm after excitation at 488 nm, and the diameter of the nanocrystals is approximately 20 nm according to the manufacturer's specifications.

Several parameters influenced the uniformity of the detected signal over the field of view, which depend both on the optical coupling of the laser to the microscope, the alignment of the detectors, and the variation of the detection efficiency of the SPADs of the matrix. This parameter is, therefore, the product between the uniformity of the excitation intensity obtained by the DOE, the coupling efficiency between the excitation volumes and the SPAD, and the PDE of the SPADs. Fig. 3 shows the measured uniformity of the system normalized by its mean value after dark counts subtraction. More than 70% of the pixels have a uniformity within 15% of the mean value. The largest deviations of about 30%, which were caused by an uneven illumination of the DOE by the Gaussian laser beam, were obtained at the outer rim of the array. The measured overall uniformity was sufficient for the proposed applications.

Additionally, we tested the linearity of the *gate width* (Fig. 4), i.e. how precisely *gate width* could be set by the FPGA device. A stabilized LED was placed in front of the sensor, and image sequences at variable *gate widths* between 1 ns and 20 ns were acquired. Considering that the illumination intensity was constant, a signal dependent on the width of the gate was measured. Fig. 4 shows the estimated *gate width* as a function of the expected value programmed by the control software. One can observe that the width of the gate is well approximated by a linear model over a large temporal range. Below 1.5 ns and above 18 ns, deviations from linearity were observed. Indeed, the gate pulses become too short to efficiently enable and disable the LFSR counters. The obtained *gate width* range is definitely sufficient for most FLIM experiments.

B. Fluorescence Lifetime Imaging Microscopy

The multifocal FLIM-FCS setup was applied to measure the lifetime of known fluorophores both in solution and in live cells and compared to previously published values. In order to estimate the lifetime (τ, eq. 3) precisely, *gate width* was set to the minimum value of about 1.5 ns and shifted by steps of 180 ps. The exposure time of the camera for each gate shift was about 100 ms, and a total acquisition time per FLIM image of 10 s was obtained. Before each image acquisition, a dark frame at exactly the same camera setting was acquired to perform reliable background subtraction. The laser intensity on the object plane was set to values between 5 and 500 $\mathrm{mW/cm^2}$ depending on the brightness of the sample. Rhodamine 6G was dissolved in water at the concentration of 10 µM, and excited by pulsed laser light at 473 nm. A gradient in the illumination intensity (Fig. 5-a) was artificially generated to measure a variable number of photons per pixel over the field of view. A subset of the images was selected and the fit algorithm based on eq. 1 was applied to each pixel. A systematic deviation of the measured fluorescence intensity was present for less than 10% of the array detectors, which showed the highest dark counts levels. In fact, background subtraction becomes less accurate at very high counting rates due to saturation of the number of detected photons caused by the pixel dead-time.

The measured average lifetime over all the pixels was 3.8 ns $\pm$ 0.3 ns. This value is consistent with previously published results [34]. The distribution of the average lifetime over the field of view is uniform although the uneven illumination (Fig. 5-b). This is expected because the estimated lifetimes must be independent from the number of detected photons per pixel.

Afterwards, we investigated living Human Embryonal Kidney (HEK293-T) cells expressing the enhanced Green Fluorescent Protein (eGFP) [35]. The cells were plated in 35 mm petri dishes with a 150 µm glass bottom (Ibidi, Munich, Germany), cultured in Dulbecco's modified Eagle's medium without phenol red, supplemented with 10% fetal calf serum, 2 mM L-glutamine and 100 µ/ml penicillin/streptomycin and grown to about 70% confluence at 37 °C in a cell culture incubator at 5% CO_2 in water-saturated air. Subsequently, cells were transfected with eGFP cDNA in plasmid vector pEGFP-N1 (Clontech, Saint-Germain-en-Laye, France) using

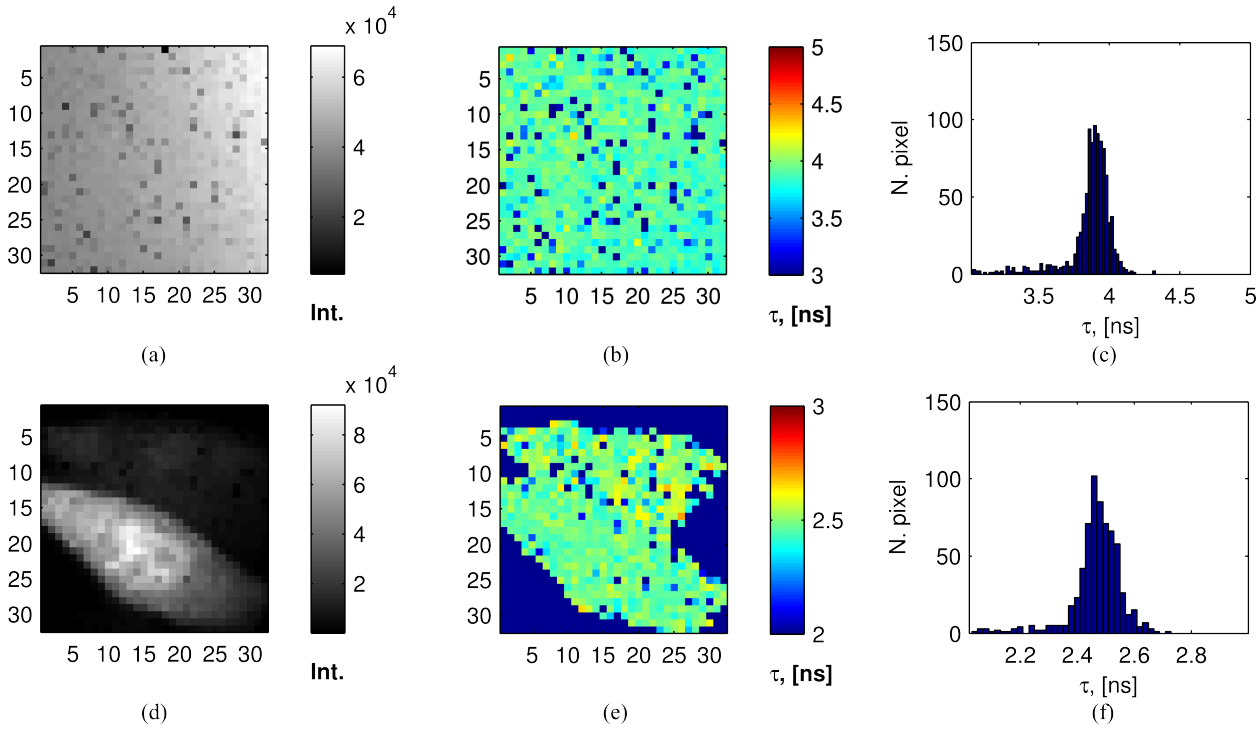

Figure 5. (a) Fluorescence emission of Rhodamine 6G under gradient illumination. (b) FLIM image and (c) histogram of the estimated average lifetimes of the same Rhodamine solution. (d) Fluorescence emission of two HEK293-T cells with different eGFP expression levels. (e) FLIM image and (f) histogram of the estimated average lifetimes of the same cells.

Lipofectamine 2000 (Life Technologies, Darmstadt, Germany) as transfection reagent according to the manufacturer's instructions. Transfected cells were used for microscopy within 48 hours. Fig. 5-c shows the intensity image of two HEK293-T cells at variable expression levels of the protein. The decay dynamics of eGFP is known to be multi-exponential both when expressed in living systems and in solutions of the isolated protein [36], [37], depending e.g. on pH or the refractive index of the solvent. Precise modeling of the fluorescence decay kinetic of this type of fluorescent molecules requires time-correlated single photon counting instrumentation with a temporal resolution of few tens of picoseconds. The fluorophore exists, indeed, in a protonated form which decays with a time constant of 250 ps [36]. Despite that, it is still possible to measure the average lifetime of eGFP using time-gated techniques, even though the shortest gate achievable is above one nanosecond [38]. The average and standard deviation of the estimated lifetimes for both cells in Fig. 5-c,d was 2.4 $\pm$ 0.13 ns, which is very similar to the results from previous investigations [36]. The deviation of the measured lifetimes around the mean value is due to statistical fluctuations of the detected photons and not by a heterogeneity of the observed sample. It must be observed that the acquisition time of the FLIM images were limited by the available laser power and by the used gate settings rather than by the performance of the camera. The presented camera is capable of collecting 2-gate FLIM images within 25 to 50 µs, depending on the clock frequency. This exposure time is calculated as twice the shortest acquisition time for the single frame (10.37 to 20.74 µs) and the update time of the DLLs inside the FPGA. However, reliable FLIM experiments under this operating condition would require an optimization of the gate intervals, the repetition rate and power of the pulsed laser source which are outside the scope of the current work. Compared with standard FLIM techniques, Time correlated single photon counting experiments, both based on point detectors or coded-anode photomultipliers, outperform the presented camera in term of the accuracy and resolution of the measured lifetimes. But the presented system is capable of measuring FCS in 1024 regions of the sample, additionally to the lifetime of the fluorophores, in a single experiment.

C. Fluorescence Correlation Spectroscopy

The multifocal microscope was applied to measure the diffusion of single fluorophores in solution. We have chosen QD because of their brighter emission and slower diffusion time compared to Rhodamine 6G, which is typically used for the calibration of FCS setups. The probe was prepared as described in section V-A. The sample was illuminated by an average laser power of about 25 µW per excitation volume. Raw FCS data collected by the camera consisted of 130.000 frames acquired every 20.74 µs, yielding 1024 fluorescence intensity fluctuation traces recorded over 2.7 s. The average count-rate per pixel was about 30 kcps.

The concentration of the fluorophores in various runs was slightly different, but always between 0.05 nM and 2 nM, as verified by FCS using a conventional instrument (ConfoCor 3, Zeiss, Jena, Germany).

Fig. 6-a,b show the values of the estimated τ_D and G_0 for each pixel respectively. These images appear to be noisy because they has contribution from fluctuations generated by

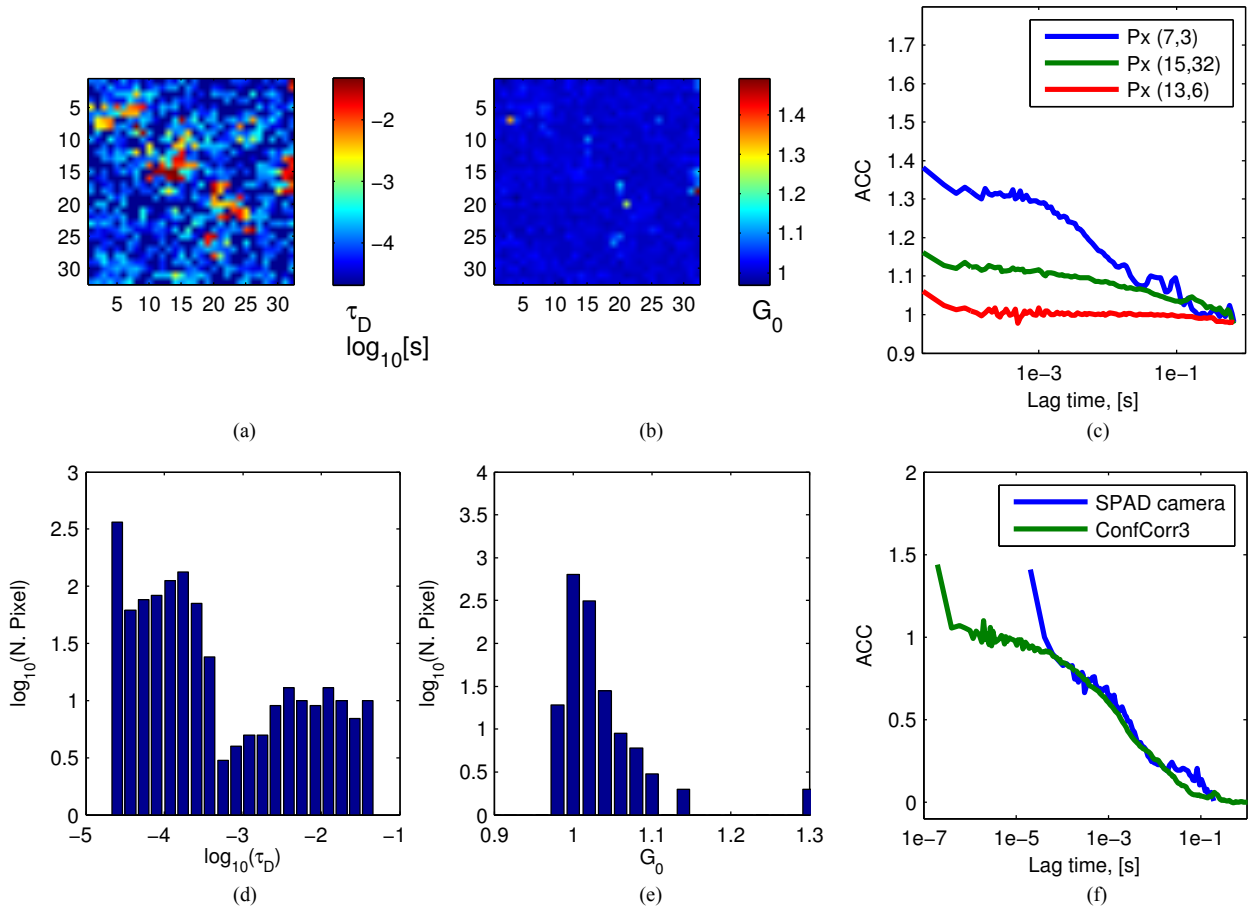

Figure 6. Plot of the estimated τ_D (a) and G_0 (b) values over the whole field of view and calculated histograms (d) and (e). (c) Measured ACC of selected pixels. (f) Comparison between the measured ACC by the SPAD camera and by Zeiss ConfoCor 3 microscope.

single quantum dots movement, characterized by a diffusion time $\tau_D \approx 600\mu$s, and quantum dot agglomerates that are slowly diffusing, $\tau_D \approx 3 - 30$ ms, and are readily visualized because of their relatively higher brightness. This is evident from the diffusion time distribution histogram in Fig. 6-d, which shows a bimodal distribution that is characteristic of the presence of fast and slowly moving fluorophores. The measured values are similar to those reported by other works [39].

Fig. 6-c shows the ACC curves of selected pixels. The green and blue traces show the typical ACC of freely diffusing fluorophores in solution. The measured ACC do not substantially differ from those measured by the commercial ConfoCor 3 microscope, although the shortest lag time for the SPAD camera has a much longer duration (Fig. 6-f). One should observe that all the ACC of Fig. 6-b have a peak at lag times below 100 µs. These peaks are due to a long-afterpulsing process, which is present for SPADs produced by the used standard CMOS process, and which generates correlated detection events on the microsecond time scale. The ACC of one of the selected pixels (red trace, Fig. 6-b) shows a dominant afterpulsing contribution. The presence of afterpulsing was verified by cross-correlating the measured signal of neighboring pixels after uniform illumination of the camera. While the ACC show the peak for short lag-times, the cross-correlation curve was statistically spread around one (data not shown). The autocorrelation peak present in Fig. 6-c would be removed by implementing more advanced correlation techniques as Fluorescence Cross-Correlation Spectroscopy (FCCS). This would however require the parallel acquisition of the fluorescence emission signal by two identical SPAD cameras.

At present, the dominant noise sources in the FCS measurements shown in Fig. 6 are the afterpulsing and dark-counts generation processes, which systematically affect the absolute value of G_0 and, therefore, perturbs the quantitative analysis. However, since most of the afterpulsing contribution vanishes within 1 µs [19], the effect of afterpulsing on diffusion times of individual quantum dots and quantum dot agglomerates, which are in the order of 600 µs and 3-30 ms, respectively, is not significant.

VI. Conclusions

We presented a 32×32 SPAD based camera which is suitable for multifocal microscopy. This device has not only a very high frame rate, short dead-time and single photon sensitivity, but also a fast gating unit, which activates the counting of the photons in individual pixels for short intervals down to 1.5 ns. Both FCS, FLIM and standard confocal imaging are possible on the same multifocal microscope. The device has been used to accurately measure the translational diffusion time of QD in solution and the fluorescence decay kinetics of eGFP in living HEK293-T cells.

Future improvements of the current experimental setup will focus on the observation of single molecules in solutions and in live cells, and on the real-time processing of FCS and FLIM data by the acquisition electronics. Additionally, further investigations are required to improve the photodetectors by reducing the dark-count rate and afterpulsing probability.

Acknowledgments

The authors thank N. Tavraz for the preparation of the HEK293-T cell cultures; G. Simmerle and A. Veronese for the excellent technical assistance. We gratefully acknowledge the support from the Federal Ministry of Education and Research (BMBF, project Quantum, FKZ 13N10067) to T. Friedrich and F.-J. Schmitt; Knut and Alice Wallenberg Foundation (grant KAW 2011.0218) to V. Vukojević; the Rajko and Maj Dermanović Fund to A. J. Krmpot. COST is acknowledged for support in the framework of the MP1205 action.

References

[1] J. Pawley, *Handbook of Biological Confocal Microscopy, 3rd Edition.* New York: Plenum Press, 2006.

[2] G. Y. Fan, H. Fujisaki, A. Miyawaki, R. K. Tsay, R. Y. Tsien, and M. H. Ellisman, "Video-rate scanning two-photon excitation fluorescence microscopy and ratio imaging with Cameleons." *Biophys J*, vol. 76, no. 5, pp. 2412–2420, 1999. [Online]. Available: http://dx.doi.org/10.1016/S0006-3495(99)77396-0

[3] L. Greenbaum, C. Rothmann, R. Lavie, and Z. Malik, "Green fluorescent protein photobleaching: a model for protein damage by endogenous and exogenous singlet oxygen." *Biol. Chem.*, vol. 381, no. 12, pp. 1251–1258, Dec 2000. [Online]. Available: http://dx.doi.org/10.1515/BC.2000.153

[4] E. Wang, C. M. Babbey, and K. W. Dunn, "Performance comparison between the high-speed Yokogawa spinning disc confocal system and single-point scanning confocal systems." *J Microsc*, vol. 218, no. 2, pp. 148–159, 2005. [Online]. Available: http://dx.doi.org/10.1111/j.1365-2818.2005.01473.x

[5] R. Rigler, *FCS in Single molecule analysis. Nobel Symposium on Single molecule spectroscopy in chemistry, physics and biology.* Springer, New York, 2010.

[6] A. Rochas, M. Gosch, A. Serov, P. Besse, R. Popovic, T. Lasser, and R. Rigler, "First fully integrated 2-D array of single-photon detectors in standard CMOS technology." *Photonics Technology Letters, IEEE*, vol. 15, no. 7, pp. 963–965, 2003.

[7] F. Guerrieri, S. Tisa, A. Tosi, and F. Zappa, "Two-dimensional SPAD imaging camera for photon counting." *IEEE Photonics Journal*, vol. 2, no. 5, pp. 759–774, 2010.

[8] M. Gersbach, J. Richardson, E. Mazaleyrat, S. Hardillier, C. Niclass, R. Henderson, L. Grant, and E. Charbon, "A low-noise single-photon detector implemented in a 130 nm CMOS imaging process." *Solid-State Electronics*, vol. 53, no. 7, pp. 803–808, 2009. [Online]. Available: http://www.sciencedirect.com/science/article/pii/S0038110109000896

[9] H. Blom, M. Johansson, A.-S. Hedman, L. Lundberg, A. Hanning, S. Hård, and R. Rigler, "Parallel fluorescence detection of single biomolecules in microarrays by a diffractive-optical-designed 2×2 fan-out element." *Appl. Opt.*, vol. 41, no. 16, pp. 3336–3342, 2002. [Online]. Available: http://ao.osa.org/abstract.cfm?URI=ao-41-16-3336

[10] H. Blom, M. Johansson, M. Gösch, T. Sigmundsson, J. Holm, S. Hård, and R. Rigler, "Parallel flow measurements in microstructures by use of a multifocal 4×1 diffractive optical fan-out element." *Appl. Opt.*, vol. 41, no. 31, pp. 6614–6620, 2002. [Online]. Available: http://ao.osa.org/abstract.cfm?URI=ao-41-31-6614

[11] M. Gösch, A. Serov, T. Anhut, T. Lasser, A. Rochas, R. S. Popovic, H. Blom, and R. Rigler, "Parallel single molecule detection with a fully integrated single-photon 2×2 cmos detector array." *Journal of Biomedical Optics*, vol. 9, no. 5, pp. 913–921, 2004.

[12] X. Michalet, R. A. Colyer, G. Scalia, T. Kim, M. Levi, D. Aharoni, A. Cheng, F. Guerrieri, K. Arisaka, J. Millaud, I. Rech, D. Resnati, S. Marangoni, A. Gulinatti, M. Ghioni, S. Tisa, F. Zappa, S. Cova, and S. Weiss, "High-throughput single-molecule fluorescence spectroscopy using parallel detection." *Proc Soc Photo Opt Instrum Eng*, vol. 7608, no. 76082D, 2010. [Online]. Available: http://dx.doi.org/10.1117/12.846784

[13] J. Buchholz, J. W. Krieger, G. Mocsár, B. Kreith, E. Charbon, G. Vámosi, U. Kebschull, and J. Langowski, "FPGA implementation of a 32×32 autocorrelator array for analysis of fast image series." *Opt Express*, vol. 20, no. 16, pp. 17 767–17 782, 2012.

[14] X. Michalet, R. A. Colyer, G. Scalia, A. Ingargiola, R. Lin, J. E. Millaud, S. Weiss, O. H. W. Siegmund, A. S. Tremsin, J. V. Vallerga, A. Cheng, M. Levi, D. Aharoni, K. Arisaka, F. Villa, F. Guerrieri, F. Panzeri, I. Rech, A. Gulinatti, F. Zappa, M. Ghioni, and S. Cova, "Development of new photon-counting detectors for single-molecule fluorescence microscopy." *Philos Trans R Soc Lond B Biol Sci*, vol. 368, no. 1611, p. 20120035, 2013. [Online]. Available: http://dx.doi.org/10.1098/rstb.2012.0035

[15] M. Kloster-Landsberg, D. Tyndall, I. Wang, R. Walker, J. Richardson, R. Henderson, and A. Delon, "Note: multi-confocal fluorescence correlation spectroscopy in living cells using a complementary metal oxide semiconductor-single photon avalanche diode array." *Rev Sci Instrum*, vol. 84, no. 7, p. 076105, 2013. [Online]. Available: http://dx.doi.org/10.1063/1.4816156

[16] A. Draaijer, R. Sanders, and H. C. Gerritsen, "Fluorescence lifetime imaging, a new tool in confocal microscopy," in *Handbook of biological confocal microscopy*. Springer, 1995, pp. 491–505.

[17] C. J. de Grauw and H. C. Gerritsen, "Multiple time-gate module for fluorescence lifetime imaging," *Appl. Spectrosc.*, vol. 55, no. 6, pp. 670–678, Jun 2001.
[18] T. W. J. Gadella, Ed., *FRET and FLIM Techniques, Volume 33*. Amsterdam: Elsevier Science, 2008.
[19] S. Tisa, A. Tosi, and F. Zappa, "Fully-integrated CMOS single photon counter." *Opt Express*, vol. 15, no. 6, pp. 2873–2887, 2007.
[20] F. Guerrieri, S. Tisa, and F. Zappa, "Fast single-photon imager acquires 1024 pixels at 100 kframe/s." in *SPIE: Sensors, Cameras, and Systems for Industrial/Scientific Applications X*, 2009.
[21] S. Cova, M. Ghioni, A. Lacaita, C. Samori, and F. Zappa, "Avalanche photodiodes and quenching circuits for single-photon detection." *Appl Opt*, vol. 35, no. 12, pp. 1956–1976, 1996.
[22] S. Tisa, F. Guerrieri, and F. Zappa, "Variable-load quenching circuit for single-photon avalanche diodes." *Opt Express*, vol. 16, no. 3, pp. 2232–2244, 2008.
[23] S. P. Chan, Z. J. Fuller, J. N. Demas, and B. A. DeGraff, "Optimized gating scheme for rapid lifetime determinations of single-exponential luminescence lifetimes." *Anal Chem*, vol. 73, no. 18, pp. 4486–4490, 2001.
[24] D. D.-U. Li, S. Ameer-Beg, J. Arlt, D. Tyndall, R. Walker, D. R. Matthews, V. Visitkul, J. Richardson, and R. K. Henderson, "Time-domain fluorescence lifetime imaging techniques suitable for solid-state imaging sensor arrays." *Sensors*, vol. 12, no. 5, pp. 5650–5669, 2012. [Online]. Available: http://dx.doi.org/10.3390/s120505650
[25] P. Hall and B. Selinger, "Better estimates of exponential decay parameters." *J. Phys. Chem.*, vol. 85, no. 20, pp. 2941–2946, 1981. [Online]. Available: http://pubs.acs.org/doi/abs/10.1021/j150620a019
[26] J. Tellinghuisen and C. W. Wilkerson, "Bias and precision in the estimation of exponential decay parameters from sparse data." *Anal. Chem.*, vol. 65, no. 9, pp. 1240–1246, 1993. [Online]. Available: http://dx.doi.org/10.1021/ac00057a022
[27] M. Maus, M. Cotlet, J. Hofkens, T. Gensch, F. C. de Schryver, J. Schaffer, and C. A. Seidel, "An experimental comparison of the maximum likelihood estimation and nonlinear least-squares fluorescence lifetime analysis of single molecules." *Anal. Chem.*, vol. 73, no. 9, pp. 2078–2086, 2001.
[28] K. Schätzel, M. Drewel, and S. Stimac, "Photon correlation measurements at large lag times: Improving statistical accuracy." *J. Mod. Opt.*, vol. 35, no. 4, pp. 711–718, 1988. [Online]. Available: http://www.informaworld.com/10.1080/09500348814550731
[29] T. Wohland, R. Rigler, and H. Vogel, "The standard deviation in fluorescence correlation spectroscopy." *Biophys J*, vol. 80, no. 6, pp. 2987–2999, 2001. [Online]. Available: http://dx.doi.org/10.1016/S0006-3495(01)76264-9
[30] J. R. Lakowicz, *Principles of Fluorescence Spectroscopy.*, 3rd ed. Springer, New York, 2006.
[31] S. R. Aragon and R. Pecora, "Fluorescence correlation spectroscopy as a probe of molecular dynamics." *The Journal of Chemical Physics*, vol. 64, no. 4, pp. 1791–1803, 1976. [Online]. Available: http://dx.doi.org/10.1063/1.432357
[32] D.-U. Li, E. Bonnist, D. Renshaw, and R. Henderson, "On-chip, time-correlated, fluorescence lifetime extraction algorithms and error analysis." *J Opt Soc Am A Opt Image Sci Vis*, vol. 25, no. 5, pp. 1190–1198, 2008.
[33] D.-U. Li, J. Arlt, J. Richardson, R. Walker, A. Buts, D. Stoppa, E. Charbon, and R. Henderson, "Real-time fluorescence lifetime imaging system with a 32×32 0.13 μm CMOS low dark-count single-photon avalanche diode array." *Opt Express*, vol. 18, no. 10, pp. 10 257–10 269, 2010.
[34] R. Reisfeld, R. Zusman, Y. Cohen, and M. Eyal, "The spectroscopic behaviour of rhodamine 6G in polar and non-polar solvents and in thin glass and PMMA films." *Chemical physics letters*, vol. 147, no. 2, pp. 142–147, 1988.
[35] G. Zhang, V. Gurtu, and S. R. Kain, "An enhanced green fluorescent protein allows sensitive detection of gene transfer in mammalian cells." *Biochem. Biophys. Res. Commun.*, vol. 227, no. 3, pp. 707–711, 1996. [Online]. Available: http://dx.doi.org/10.1006/bbrc.1996.1573
[36] M. Cotlet, J. Hofkens, M. Maus, T. Gensch, M. van der Auweraer, J. Michiels, G. Dirix, M. van Guyse, J. Vanderleyden, A. J. W. G. Visser, and F. de Schryver, "Excited-state dynamics in the enhanced green fluorescent protein mutant probed by picosecond time-resolved single photon counting spectroscopy." *J. Phys. Chem. B*, vol. 105, no. 21, pp. 4999–5006, 2001. [Online]. Available: http://pubs3.acs.org/acs/journals/doilookup?in_doi=10.1021/jp003813i
[37] M. Vitali, F. Picazo, Y. Prokazov, A. Duci, E. Turbin, C. Götze, J. Llopis, R. Hartig, A. J. W. G. Visser, and W. Zuschratter, "Wide-field multi-parameter FLIM: Long-term minimal invasive observation of proteins in living cells." *PloS ONE*, vol. 6, no. 2, pp. e15 820–, 2011. [Online]. Available: http://dx.doi.org/10.1371%2Fjournal.pone.0015820
[38] H. C. Gerritsen, M. A. H. Asselbergs, A. V. Agronskaia, and W. G. J. H. M. van Sark, "Fluorescence lifetime imaging in scanning microscopes: acquisition speed, photon economy and lifetime resolution." *J. Microsc.*, vol. 206, no. 3, pp. 218–224, 2002. [Online]. Available: http://dx.doi.org/10.1046/j.1365-2818.2002.01031.x
[39] Y. Han, J. Lee, Y. Lee, and S. W. Kim, "Measurement of the diffusion coefficients of fluorescence beads and quantum dots by using fluorescence correlation spectroscopy." *Journal of the Korean Physical Society*, vol. 59, no. 5, pp. 3177–3181, 2011.

Marco Vitali received the M.Sc. degree in Electronic Engineering from Politecnico di Milano in 2006, and the Ph.D. degree with summa cum laude at the Berlin Institute of Technology in 2011. His main research interests are fluorescence lifetime imaging microscopy of living cells and the development of bidimensional single photon timing detectors as position-sensitive photomultipliers and SPAD arrays. He is currently working as hardware engineer in the company Omicron Energy Solutions GmbH in Berlin.

Danilo Bronzi obtained the B.Sc. degree cum laude in biomedical engineering at Politecnico di Milano, Italy, in 2008 and the M.Sc. degree cum laude in electronic engineering at Politecnico di Milano, in July 2011. Since October 2011 he has been enrolled in the Ph.D. program in the Department of Electronics, Information and Bioengineering at Politecnico di Milano. His current research activity focuses on the design and development of novel CMOS single-photon sensors for 2-D and 3-D imaging applications.

Aleksandar J. Krmpot , research associate in Institute of physics, University of Belgrade, Serbia received Ph.D. degree in quantum optics at University of Belgrade in 2010. During M.Sc. and Ph.D studies he was investigating the evolution of the coherently prepared atoms traversing different laser beams profiles. His main research activities are quantum optics and biophotonics. His current research activities are development and application of nonlinear microscopy for biohotonics structures studies in Institute of physics, Belgrade, Serbia and multifocal correlation microscopy for studies of molecular diffusion dynamics in Karolinska Institute, Stockholm, Sweden.

Stanko Nikolić obtained the B.Sc. degree in experimental physics at Faculty of Physics, University of Belgrade in 2007, and the M.Sc. degree in quantum optics at the same institution in 2008. From 2007, he has been working at Institute of Physics as a Research Assistant in the field of experimental quantum optics. Since November 2008, he has been enrolled in the Ph.D. program at Faculty of Physics, University of Belgrade in the field of electromagnetically induced transparency and slow light in Rb buffer gas cells. He is also an external collaborator at Karolinska Institute at Stockholm, with activities focused on laboratory software development.

Franz-Josef Schmitt is PostDoc at the institute of physical chemistry at the Berlin institute of technology since 2011 where he finished his doctoral thesis in physics. His research focuses on the spectroscopy of pigment-pigment and pigment-protein interactions in photosynthesis and molecular biology. He published about 40 peer reviewed articles. He is currently substitutional management committee member of COST action MP 1205.

Cornelia Junghans obtained her diploma degree in physics at the Berlin Institute of Technology in 2011. Since September 2011 she is working at the Department of Biophysical Chemistry of the same university as PhD student. Her main research interests are fluorescence spectroscopy of genetically-encoded photoswitchable fluorophores and microscopy techniques such as confocal microscopy, fluorescence recovery after photobleaching and lifetime imaging microscopy.

Simone Tisa was born in Milano, Italy, in 1977. He received the M.Sc. degree in Electronic Engineering from Politecnico di Milano in 2001, and the Ph.D. degree from the same university in 2006. He is now product R&D manager for electronics design and system integration at Micro Photon Devices. In 2008 he pioneered the first monolithic 2D SPAD imager of 32x32 pixels. His main research interests are in the field of single-photon imaging and single-photon timing of fast phenomena, by means of fully integrated arrays of SPADs and associated microelectronics.

Thomas Friedrich was born in 1965, gained a Diploma degree in Physics from University of Heidelberg in 1992 and his PhD in Biochemistry in 1997 at the University of Frankfurt/Main. After two PostDoc positions at the Center of Molecular Neurobiology in Hamburg and the Max-Planck-Institute of Biophysics he became head of the Junior Research Group Microfluidics and Biosensors at the Technical University of Ilmenau/Thuringia. Since 2006 he is full professor of Physical Chemistry at Berlin institute of technology. His research deals with electrophysiological investigations of ion transporters or ion channels in cellular membranes and fluorescence lifetime imaging microscopy to analyze bioenergetic processes. He is coauthor of about 66 papers, published in peer-reviewed journals of the biophysics and biochemistry field.

Vladana Vukojević was born in Belgrade (Serbia) 1965. She commenced her research career at the H. C. Ørsted Institute, Copenhagen, Denmark in 1989, and her academic career at the Faculty of Physical Chemistry, University of Belgrade, Serbia, where she was Associate Professor of Biophysical Chemistry until 2005. Since 2011 she is Associate Professor of Biochemistry at the Karolinska Institute, Stockholm, Sweden. Her research focuses on self-organization of dynamical systems. She uses fluorescence microscopy imaging and correlation spectroscopy to identify and quantitatively characterize in live cells self-regulatory mechanisms underlying vital biological functions such as gene transcription and cellular signaling. She is coauthor of more than 50 papers published in peer-reviewed journals.

Lars Terenius was born in Örebro (Sweden) in 1940. He was appointed Professor in Pharmacology at Uppsala University in 1976 and resigned 1988 for a visiting scientist scholarship at the National Institutes of Health in Bethesda, MD (USA). He was appointed Professor at the Karolinska Institutet 1989. His research is focused on molecular mechanisms of pathology ranging from cancer to chronic pain and drug/alcohol dependence. He is also Founding Director of Center for Molecular Medicine (CMM) a research center at the Karolinska University Hospital with over 300 scientists. His recent work in collaboration with Professor Rudolf Rigler is imaging of molecules in the living cell using fluorescence correlation spectroscopy (FCS). This research has required modification or new constructions of apparatus, to acquire single molecule sensitivity and high temporal and spatial resolution. He has published over 500 papers in peer-reviewed periodicals.

Franco Zappa was born in Milano (Italy) in 1965. Since 2011 he is full professor of Electronics at Politecnico di Milano. His research deals with microelectronic circuitry for single-photon detectors (SPAD) and CMOS SPAD imagers, for high-sensitivity time-resolved measurements, 2D imaging and 3D depth ranging. He is coauthor of about 130 papers, published in peer-reviewed journals and in conference proceedings, and 9 text books on Electronic Design and Electronic Systems. He is co-author of 4 international patents. From 2007 he is Senior Member IEEE. In 2004 he co-founded “Micro Photon Devices” focused on the production of SPAD modules for single photon-counting and photon-timing.

Rudolf Rigler was born in Franfurt/Main Germany, 1936. MD 1960, University Graz,Austria, PhD 1966, Karolinska Institute Stockholm, Sweden. Postdoctoral fellow with Manfred Eigen (Nobel laureate in chemistry) 1967-1970. Professor in Molecular and Medical Biophysics at the Karolinska Institutet 1976-2001. Professeur invite at the Swiss Federal Institute of Technology Lausanne (EPFL) 2001-2011. Member of the Nobel Assembly of the Karolinska Institutet. Member of the Royal Swedish Acedemy of Sciences (KVA), the Royal Engeneering Science Academy (IVA), the Leopoldina, a.o. In RRs laboratory Fluorescence Correlation Spectroscopy, Confocal Single Molecule Detection and Wide Field Imaging were developed. He has published more than 200 scientific papers, he is inventor of 40 patents and Cofounder of Evotec AG, Germany, Gnothis AG and Biophos AG both Switzerland.